Colloids and Surfaces A 538 (2018) 127–132

Contents lists available at ScienceDirect

Colloids and Surfaces A

journal homepage: www.elsevier.com/locate/colsurfa

Defect-free exfoliation of graphene at ultra-high temperature

Mahmoud M.M. Ahmed[a], Toyoko Imae[a,b,*], Jonathan P. Hill[c], Yusuke Yamauchi[c,d], Katsuhiko Ariga[c,e], Lok Kumar Shrestha[c,**]

[a] Graduate Institute of Applied Science and Technology, National Taiwan University of Science and Technology, 43 Section 4, Keelung Road, Taipei 10607, Taiwan
[b] Department of Chemical Engineering, National Taiwan University of Science and Technology, 43 Section 4, Keelung Road, Taipei 10607, Taiwan
[c] World Premier International Center for Materials Nanoarchitectonics (WPI-MANA), National Institute for Materials Science (NIMS), 1-1 Namiki, Tsukuba 305-0044, Japan
[d] School of Chemical Engineering & Australian Institut for Bioengineering and Nanotechnology (AIBN), The University of Queenland, Brisbane, QLD 4072, Australia
[e] Graduate School of Frontier Science, The University of Tokyo, Kashiwa 277-0827, Japan

GRAPHICAL ABSTRACT

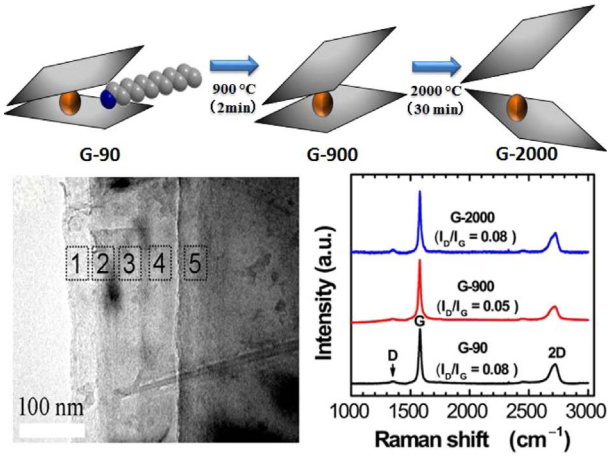

ARTICLE INFO

Keywords:
Graphene
$FeCl_3$-graphite intercalation compound
Ultra-high temperature treatment
Defect-free graphene exfoliation
Graphene sp^2 sheet
Specific capacitance increment

ABSTRACT

We report the effect of treatment at high temperature (2000 °C) on the exfoliation of a graphene that had been prepared by amine-treatment of an $FeCl_3$-graphite intercalation compound and by preheat-treatment at low temperature (900 °C). A well expanded morphology was produced by the exfoliation, and the expansion did not lead to significant defects in the graphene sp^2 sheet after heating at 2000 °C. The exfoliated graphene also exhibited an enhanced capacitance. It should be noted that this heat-treatment method at ultra-high temperature provides a physical procedure for defect-free graphene exfoliation following the electrochemical performance.

* Corresponding author at: Graduate Institute of Applied Science and Technology, National Taiwan University of Science and Technology, 43 Section 4, Keelung Road, Taipei 10607, Taiwan.
** Corresponding author at: World Premier International Center for Materials Nanoarchitectonics (WPI-MANA), National Inatitute for Materials Science (NIMS), 1-1 Namiki, Tsukuba 305-0044, Japan.
E-mail addresses: imae@mail.ntust.edu.tw (T. Imae), SHRESTHA.Lokkumar@nims.go.jp (L.K. Shrestha).

http://dx.doi.org/10.1016/j.colsurfa.2017.10.074
Received 8 September 2017; Received in revised form 24 October 2017; Accepted 28 October 2017
Available online 28 October 2017
0927-7757/

1. Introduction

Graphene exfoliation has become hot research topics in the field of nanocarbon materials after the Scotch™ tape method was discovered [1]. Exfoliated graphene possesses unique optoelectronic properties and offers excellent prospects for practical applications leading to a necessity for the development of suitable scalable methods for its production [2,3]. As with other nanomaterials, top-down methods are commonly used for graphite exfoliation. Physical and chemical routes have been developed to obtain highquality graphene layers. Physical routes usually involve the use of Hansen solubility parameters with mechanical exfoliation in different aqueous/organic media [4]. Although they yield graphenes with relatively high-quality, the yields are rather low and require improvement [5]. Incidentally, Hummers' method has been widely used for chemical exfoliation [6] and these methods have been developed to produce graphenes with improved quality [7,8].

On the other hand, graphite intercalated compound (GIC) research has become a fascinating popular field of investigation [9,10]. The intercalated (donor/acceptor) compounds might be used to provide a scalable and less-defective exfoliated graphene, which could be useful in various applications. GIC such as lithium or calcium intercalated graphites is the principal materials used for lithium ion/air batteries [11] and superconductors [12–14]. Meanwhile, potassium intercalated graphite has been exfoliated by using a strong exothermic reaction releasing hydrogen gas [15]. Most donor-type intercalated compounds ought to be susceptible to exfoliation by applying hydrogen generation reduction reactions and microwave exfoliation [16,17]. Recently, GIC exfoliation using microwave reaction has been more widely used [18]. However, this mild exfoliation process requires further improvements in terms of scalability and of optimization on the quality of the graphene produced. The excellent performances achieved for sodium ion batteries are due to a co-intercalation mechanism rather than the strong oxidative conditions [19].

Thus, the thermal exfoliation of doped graphite, GIC and other graphite composites is a widely-focused issue. That is, heat-treatment of these materials can effectively enhance graphene production and electronic properties. Well-exfoliated sulphur-doped graphene was produced after thermal annealing of graphene oxide in sulphur atmosphere [20,21]. Similarly, N, P or S-doped graphene is also exfoliated [22]. These expanded graphite composites showed better exfoliation than reduced graphite oxide and heightened electrochemical properties. The intercalated metals are thought to improve electronic properties by promoting charge transfer between graphene layers and the dopant elements [23,24]. These electronic aspects of intercalated graphene produce distinct graphene layers due to variations in the Fermi energy level. Nevertheless, exfoliation procedures performed at higher temperature increases the functionalization and defects of the graphene [25]. Therefore, producing a non-defected and well-expanded graphene is highly required.

Herein, we report the thermal expansion of amine-treated $FeCl_3$-GIC. The expansion was carried out by a physical process and could be developed as a process for graphene exfoliation. Additionally, the electrochemical performance of this expanded graphene was also tested. This expansion procedure will significantly endure graphene exfoliation through a defect-less technique.

2. Experimental section

2.1. Materials

Graphite flake powder was purchased from Ito Co., Tokyo, Japan. Dodecylamine and *N*-methylpyrrolidone were purchased from Acros Organics, Belgium. Polyvinylidene fluoride (molecular weight 275,000 by gel permeation chromatography) was obtained from Sigma Aldrich, USA. Sodium chloride was purchased from Nacalai Tesque, Japan. < opt_COMMENT > Author has rejected a copyediting change here. " < opt_COMMENT selectedText = "" > We delete " < opt_COMMENT > Author has rejected a copyediting change here. "N < opt_COMMENT > Author has rejected a copyediting change here. "N < opt_COMMENT > Author has rejected a copyediting change here. "- < opt_COMMENT > Author has rejected a copyediting change here. "" becase we modifed to be "and N-".N-We delete "N-

2.2. Thermal treatment

Amine-treatment of stage-1 $FeCl_3$-GIC and pre-heating (at 900 °C for 2 min under air atmosphere in a muffle furnace) of amine-treated graphene were performed by previously published methods [26,27]. Amine-treated and pre-heated graphene was heat-treated for 30 min at 2000 °C, which was reached at a heating rate of 25 °C/min under N_2 gas atmosphere [28], yielding the product.

2.3. Characterizations

Scanning electron microscopic (SEM) images were collected using a Hitachi S-4800 SEM operated at an accelerating voltage 5 kV with 10 μA emission current. SEM specimens were prepared on clean silicon substrates by dropping a pyridine dispersion of each sample followed by drying in air for 2 h. Specimens were sputtered with platinum metal (~2 nm) using a Hitachi S-2030 ion coater prior to SEM measurements. Raman spectroscopic analysis was performed on the powdered graphene spread on a copper stage using a Jobin-Yvon T64000 equipped with a green laser (λ = 514.5 nm, laser power = 0.1 W). Scans were performed for 10 s with 10 times accumulation using 100× magnification. Transmission electron microscopic (TEM) images and selected area electron diffraction (SAED) patterns were obtained by using a JEOL Model JEM-2100F operating at 200 kV. TEM specimens were prepared by dropping a pyridine suspension of sample (suspension condition: 3 h at 30 W) onto a standard carbon-coated copper grid followed by drying in air for 4 h. X-ray photoelectron spectroscopic (XPS) measurements were performed on a Theta Probe spectrometer (Thermo Electron Co. Germany) using monochromated Al−Kα radiation (photon energy 15 KeV, maximum energy resolution ≤ 0.47 eV, maximum space resolution ≤ 15 μm). Thermogravimetric analysis (TGA) was performed with Hitachi HT-Seiko Instrument Exter 6300 TG/DTA and Q 500 TA instrument. The specimen was heated from the ambient temperature to 1000 °C at 10.0 °C min^{-1} under air atmosphere. Nitrogen adsorption/desorption isotherms were recorded on BELSORB Max for the estimation of Brunauer–Emmett–Teller (BET) surface area.

2.4. Electrochemical measurement

Cyclic voltammetric (CV) and charge/discharge measurements at room temperature were performed in an aqueous electrolyte solution (1.0 M NaCl) on a Zahner Zennium E electrochemical workstation (model CH850D, Germany), using a three-electrode system with glassy carbon working electrode (10 mm diameter, ALS, Japan), Ag/AgCl reference electrode, and platinum wire counter electrode. For the preparation of the working electrode, samples were sonicated with polyvinylidene fluoride and *N*-methylpyrrolidone (10% binder ratio) to form a homogenous suspension, and then the suspension was dropped onto the glassy carbon electrode followed by drying at 50 °C for 12 h. The potential window range was set between 0 and 0.8 V and scan rate was varied from 5 to 500 mV s^{-1}. The specific capacitance (C_s) of the electrode materials was calculated from the CV curves using a previously reported standard equation [29]. Cyclic stability of the working electrode was tested over 20,000 charge/discharge cycles at 20 A g^{-1}.

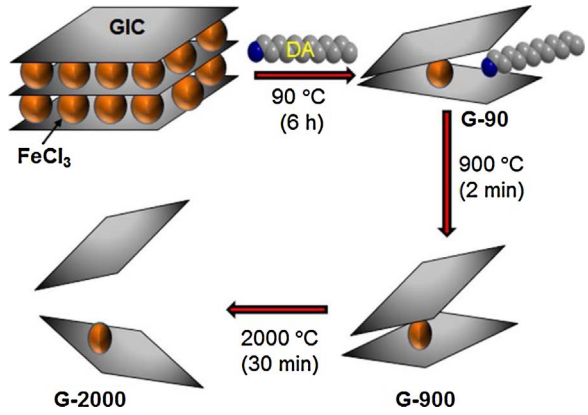

Fig. 1. Schematic representation of the production of G-2000. DA: dodecylamine.

3. Results and discussion

Amine-treated graphene (G-90), prepared from $FeCl_3$-GIC by treating with dodecylamine (DA) for 6 h at 90 °C, was heated for 2 min at 900 °C in air to produce G-900, which was then further heat-treated for 30 min at the higher temperature of 2000 °C under nitrogen atmosphere to further expand the graphene (G-2000) (Fig. 1). It could be observed from SEM images of the powder samples that each heat-treatment process caused a remarkable morphological expansion of the graphene layers (Fig. 2). The interlayer expansion increased with increasing processing temperature from G-90 to G-900 to G-2000 with G-2000 having greatest degree of homogenous expansion (Figs. 2, and S1–3). These features of expanded graphene are imperative, since the graphene is resistant against high temperatures with occurring expansion rather than combustion. Additionally, Figs. S4–6 show different magnifications of SEM and TEM images of the exfoliated graphene flakes with numerous sizes after sonication in pyridine.

Expansion caused by heat-treatment increases the volume of G-90 [27], and similar volume increases have also been observed for expanded obtained from other donor and acceptor type intercalated graphite [30], where polyethylene terephthalate, potassium permanganate and others have been utilized as intercalator compounds [31–33]. Acetic anhydride and strong oxidizing agents have also been used for the expansion procedure [34], while a more sophisticated laser irradiation procedure has been applied to sulfuric acid-intercalated graphite and sodium-intercalated expanded graphite [35]. On the other hand, acceptor type GICs including aluminium oxide-intercalated graphite obtained by a roll milling technique exhibited a similar expanded morphology [36]. This expanded graphite could be formed of uniform thin layers, a feature of which is significant for device fabrication. These processes are triggered by the presence of dopants (acids or polymer molecules), which promote the expansion behaviour of graphene. However, the majority of these previously reported expansion techniques introduced major imperfections or defects to the graphitized basal surface [37,38].

The present procedure does not lead to such faults, since the expansion is performed by heat-treatment in the absence of any aggressive chemical reagents or procedures. The expansion could be clearly observed by the presence of thin exfoliated sheets even after mild sonication in pyridine as it can be seen in the TEM image (Fig. 3a). The expansion due to an effective heating process could also be clearly observed at the edges of graphene sheets. The high resolution (HR)-TEM image (Fig. 3b) shows ultra-thin graphene sheets with clear single, double and few layers. Electron diffraction patterns of selected area also confirmed the existence of the few layered areas (Fig. 3c). Raman scattering spectra (Fig. 4) clearly indicate non-defective expansion with minimal defects even after heat-treatment of the graphene at 2000 °C:

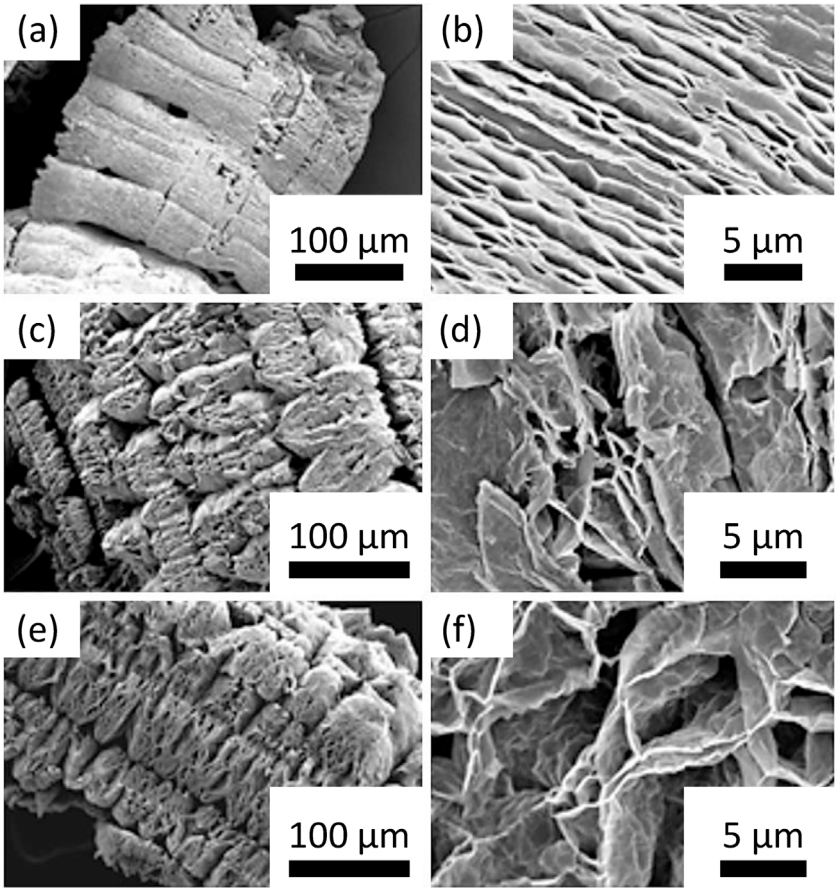

Fig. 2. SEM images of (a and b) G-90, (c and d) G-900, and (e and f) G-2000.

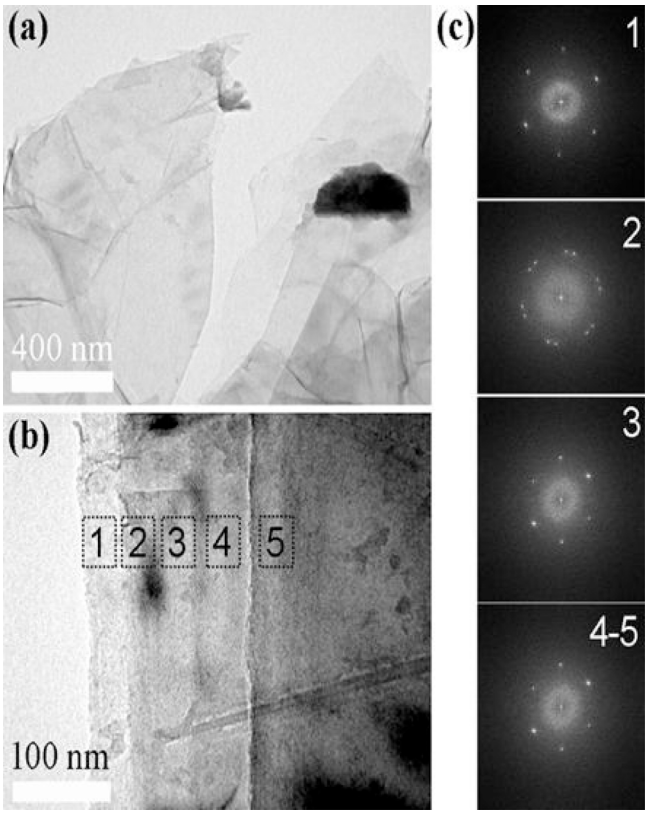

Fig. 3. (a) A TEM image of G-2000, (b) a HR-TEM image of the edge of a G-2000 sheet and (c) diffraction images of the edge of a G-2000 sheet at the position numbered in Fig. 3(b).

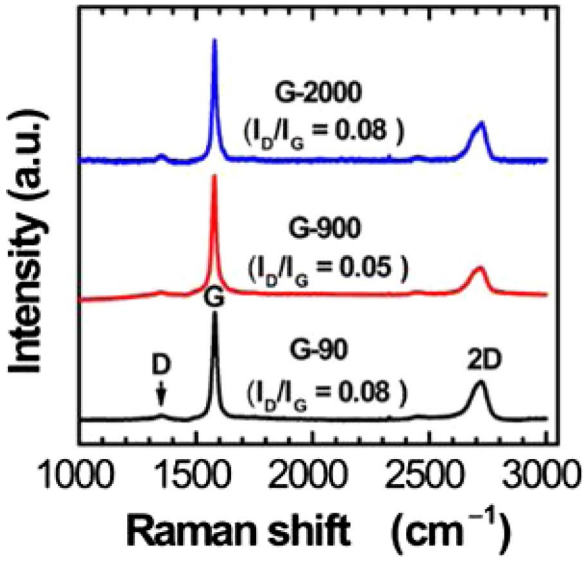

Fig. 4. Raman scattering spectra of G-90, G-900 and G-2000.

Raman spectrum of G-2000 displays mostly sp^2 carbon (G band ~1580 cm^{-1}) but the D band at ~1350 cm^{-1} corresponding to sp^3 carbon is very weak. Similar Raman data were observed for G-90 and G-900, demonstrating the fact that high-temperature treatment does not destroy the hexagonal graphitic structure. Chromium-intercalated graphene showed similar Raman behaviour with minimum defects [39], and similarly, ammonium persulfate- and potassium-intercalated graphite also induced only mild distortion and defects in the graphene surface upon expansion [9,40] despite the oxidizing power of the processing reagent. In contrast, most other exfoliation procedures result in highly-defected graphene.

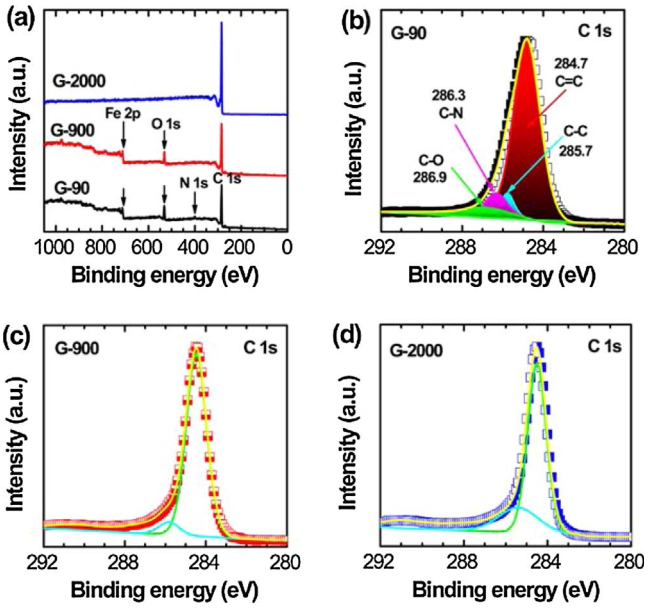

Fig. 5. (a) Corresponding XPS survey spectra and XPS core level C 1s spectrum of (b) G-90, (c) G-900 and (d) G-2000.

The I_D/I_G ratio (the area ratio of D and G Raman bands) of thermally expanded G-90 was also found to be very low when compared to graphene exfoliated by other methods. The I_D/I_G ratio of 0.05–0.08 for G-90, G-900 and G-2000 (Fig. 4) clearly indicates that the majority of carbon atoms are sp^2 but not sp^3. In contrast to N-doped graphene exfoliated by applying microwave irradiation that produced highly defected graphene oxide [41], G-2000 contained scarce defects comparable to the case of potassium-intercalated graphene and fullerene-derived carbon microtubes [28,42]. Moreover, regarding to 2D band at 2720 nm, which reflects the multiplicity of layers in graphene, the area ratio 1.38 of I_{2D}/I_G indicates that the expanded graphene is composed mostly of exfoliated-thin graphene flakes [43]. This is consistent with TEM observations (Fig. 3).

XPS survey results (Fig. 5a) showed the core level peaks for carbon (C 1s), nitrogen (N 1s), oxygen (O 1s) and iron (Fe 2p) for G-90. MGC-900 showed XPS peaks corresponding to C 1s, O 1s and Fe 2p demonstrating the loss of amine due to the heat-treatment. However, following heat-treatment at 2000 °C, only core level XPS peak corresponding to C 1s remained. An XPS C 1s peak of G-90 (Fig. 5b) was deconvoluted into four peaks at 284.7 eV (C═C: sp^2 carbon), 285.7 eV (C—C: sp^3 carbon), 286.3 eV (C—N), and 286.9 eV (C—O), and the XPS C 1 s peaks at 286.3, and 286.9 eV corresponding to C—N and C—O carbon disappeared following heat-treatment to G-900 and G-2000 (Fig. 5c and d), indicating removal of dodecylamine and contaminants.

Expansion of graphene may be accompanied by an increase in the surface area. Nitrogen adsorption/desorption curves (Fig. 6a) showed clear differences in the sorption properties with increasing heat-

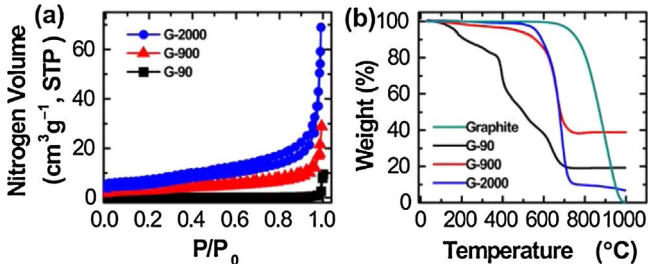

Fig. 6. (a) Nitrogen sorption isotherms of G-90, G-900, and G-2000, and (b) TGA curves of graphite, G-90, G-900, and G-2000.

treatment temperature, although G-90, G-900 and G-2000 exhibited similar Type II adsorption isotherms. The surface area of G-2000 (53 $m^2 g^{-1}$) is more than 3 times higher than that of G-900 (17 $m^2 g^{-1}$). This relatively enhanced surface area can be attributed to the interlayer expansion of graphite caused by heat-treatment. To further prove the effect on the expansion of graphene, TGA was measured under air atmosphere (Fig. 6b). Graphite showed a complete decomposition at 800–1000 °C, while G-90 was partially decomposed around 400 °C, due to the presence of amine compounds, and the decomposition of graphene occurred at 600–700 °C. Meanwhile, G-900 showed mainly the weight loss by burning of graphene at 600–700 °C after the decomposition of a small content of residual amine. which did not permit the complete decomposition of the amines present. Meanwhile, different from G-90 and G-900, G-2000 showed a complete decomposition of graphene around 600–700 °C with no organic compounds remaining. This clearly suggests that the amine compounds and other contaminants are totally decomposed by heat-treatment at 2000 °C. These results are consistent with the XPS results. TGA results indicated residues above 700 °C, where all organic and graphitic moieties were burned. These residues are iron oxide and it at 1000 °C amounted about 20, 40 and 7 wt% for G-90, G-900 and G-2000. The increase from G-90 to G-900 is attributed to the reduction of dodecylamine and the decrease from G-900 to G-2000 is due to the partial remove of iron oxide. The exfoliation of G-90 sheets were demonstrated by the disappearance of X-ray diffraction (XRD) peaks and, instead, weak small angle X-ray scattering peaks appeared [26]. Similar no-Bragg peaks in XRD patterns were observed for G-900 and G-2000 sheets (data is not shown), indicating the maintained exfoliation and no restacking on the process of heat treatment.

While the expanded graphite materials have been utilized in lithium ion batteries [44], electrochemical performances of the expanded graphene in the present investigation were studied by CV measurements using a three-electrode system. The well exfoliated graphene flakes were obtained after sonication in pyridine, as seen in Figs. S4–6, and these flakes were utilized for electrode materials. The quasi-rectangularly shaped CV curves obtained for G-900 and G-2000 are typical characteristics of an electrical double layer capacitor (EDLC) with correlated dependence on the scan rate (Fig. 7a and b). It was found that G-2000 carried a higher current than G-900, suggesting a higher specific capacitance (C_s) value. The C_s of 90 F g^{-1} obtained for G-2000

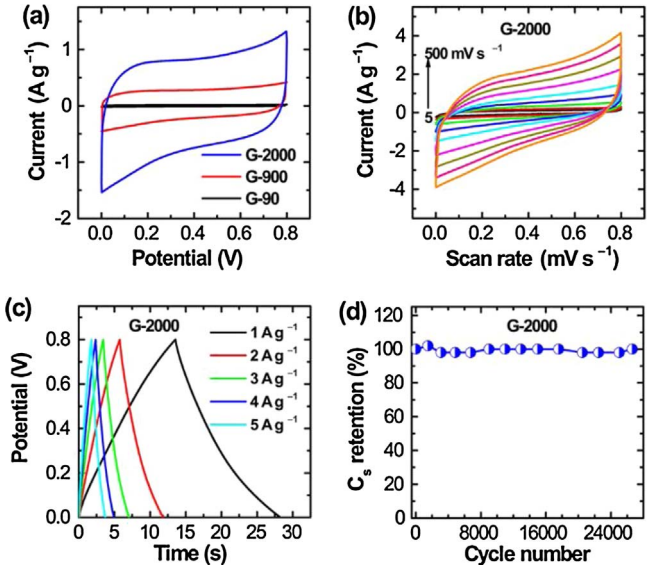

Fig. 7. (a) CV curves of G, G-900 and G-2000 versus Ag/AgCl in 1 M NaCl aqueous electrolyte at a scan rate of 50 mV s^{-1}, (b) CV curves of G-2000 at different scan rates (5–500 mV s^{-1}), (c) charge/discharge curves of G-2000 at different current densities, and (d) cyclic stability test of G-2000 at 20 A g^{-1}.

at the scan rate of 5 mV s^{-1} is 3.7 times greater than that observed for G-900, demonstrating that G-2000 is more effective as an electrode material for energy storage than G-900 (Fig. S7a). The improved supercapacitive performance of G-2000 over G-900 can be explained by the effective expansion of graphene layers in G-2000, which exhibit an electrochemically accessible surface area allowing electrolyte ions easier access to the graphene surfaces.

Charge/discharge measurements were also performed to estimate the rate capability and cyclic stability of the electrode materials. The triangular shape of charge/discharge curves (Fig. 7c), which is typical of EDLC, showed a correlated response for current densities with capacitance retention of ~54% at a high current density of 10 A g^{-1} (Fig. S7b). This demonstrates well (scan and charge/discharge) rate performances for G-2000. Additionally, the charge/discharge curves provided an ultrafast charging time of ~0.8 s. at 10 Ag^{-1}, which is suitable for emergency uninterruptable power supply devices. Keeping in mind that supercapacitor devices in real practical applications require high cyclic stability, we examined the cyclic stability of the G-2000 electrode by recording charge/discharge curves (Fig. 7d). In addition to the high rate capability described above, G-2000 showed excellent long term cyclic stability sustaining approximately 98% capacitance retention even up to 26,000 cycles at current density of 20 Ag^{-1}. Such extremely stable performance is a unique behaviour of G-2000 compared to other graphene and their composites (Table 1).

It should be noted that when fullerene crystals were heat-treated at 2000 °C, surface area increased by orders of magnitude due to the formation of large numbers of defects in the form of mesopores, since fullerene crystal was completely distorted and reformed in graphitic carbon tubes [28]. Although a similar heating procedure was performed in the present work, it produced almost defect-free graphene (without mesopore formation) maintaining the main sp^2 structure and morphology. This fact is evidently due to the effective expansion of the layered graphene structure and a resulting increase in the surface area, which allows improved accessibility for electrolyte diffusion into the electrode surface. The resulting enhanced electrochemical performance involves increasing capabilities and excellent cyclic stability.

4. Conclusions

In this work, we have prepared graphene from graphite through the expansion of dodecylamine-treated $FeCl_3$-GIC. Expansion was achieved by heat-treatment at 2000 °C for 30 min after treatment at 900 °C for 2 min without using strong acids or bases in order to avoid the introduction of disadvantageous defects to the resulting expanded graphene products. Dodecylamine was completely removed after the final heating procedure. The heat-treatment procedure of 2000 °C caused greater expansion than heat-treatment at 900 °C with the consequence that the surface area of G-2000 is three times higher than that of G-900. G-2000 showed efficient supercapacitive performance higher than that of the G-900. This novel material exhibits high rate capability as well as ultra-high cyclic stability sustaining ~98% capacitance retention after 26,000 charge/discharge cycles. The present method represents a simple method for graphene expansion/exfoliation by ultra-high

Table 1
Comparison of cyclic stability of graphene-based electrodes.

Electrode Material	Cell	Electrolyte	Conditions	Stability	Ref.
3D-G/PANI	3 electrodes	1.0 M H_2SO_4	1 Ag^{-1}	85%	[45]
G/ppy	3 electrodes	1.0 M H_2SO_4	100 mVs^{-1}	85%	[46]
Ppy/Fe oxide/ rGO	3 electrodes	1.0 M H_2SO_4	1 A g^{-1}	93%	[47]
rGO/PANI-0.1	symmetric	1.0 M H_2SO_4	4 A g^{-1}	76.5%	[48]
G-2000	3 electrodes	1.0 M NaCl	20 A g^{-1}	98%	This work

temperature treatment. It might also lead to the development of a family of new hybrid materials containing metal oxides anchored at defect-free sp^2 carbon graphene surfaces.

Acknowledgements

This work was partially supported by a grant of Ministry of Science and Technology (MOST 104-2221-E-011-003), Taiwan. Additionally, it was also supported by JSPS KAKENHI Grant Number JP16H06518 (Coordination Asymmetry) and CREST JST Grant Number JPMJCR1665, Japan. M.M.M.A. thanks the financial support from National Taiwan University of Science and Technology, Taiwan, for student scholarship and World Premier International Center for Materials Nanoarchitectonics (WPI-MANA) of National Institute for Materials Science (NIMS) for NIMS internship award.

Appendix A. Supplementary data

Supplementary data associated with this article can be found, in the online version, at http://dx.doi.org/10.1016/j.colsurfa.2017.10.074.

References

[1] K.S. Novoselov, A.K. Geim, S.V. Morozov, D. Jiang, Y. Zhang, S.V. Dubonos, I.V. Grigorieva, A.A. Firsov, Electric field effect in atomically thin carbon films, Science 306 (5696) (2004) 666–669.
[2] A.K. Geim, K.S. Novoselov, The rise of graphene, Nat. Mater. 6 (3) (2007) 183–191.
[3] R. Westervelt, Graphene nanoelectronics, Science 320 (5874) (2008) 324–325.
[4] A. Pénicaud, C. Drummond, Deconstructing graphite: graphenide solutions, Acc. Chem. Res. 46 (1) (2013) 129–137.
[5] Y. Hernandez, V. Nicolosi, M. Lotya, F.M. Blighe, Z. Sun, S. De, I.T. McGovern, B. Holland, M. Byrne, Y.K. Gun'Ko, High-yield production of graphene by liquid-phase exfoliation of graphite, Nat. Nanotechnol. 3 (9) (2008) 563–568.
[6] W.S. Hummers, R.E. Offeman, Preparation of graphitic oxide, J. Am. Chem. Soc. 80 (6) (1958) 1339–1339.
[7] D.C. Marcano, D.V. Kosynkin, J.M. Berlin, A. Sinitskii, Z. Sun, A. Slesarev, L.B. Alemany, W. Lu, J.M. Tour, Improved synthesis of graphene oxide, ACS Nano 4 (8) (2010) 4806–4814.
[8] J. Chen, Y. Li, L. Huang, C. Li, G. Shi, High-yield preparation of graphene oxide from small graphite flakes via an improved Hummers method with a simple purification process, Carbon 81 (2015) 826–834.
[9] A.M. Dimiev, G. Ceriotti, A. Metzger, N.D. Kim, J.M. Tour, Chemical mass production of graphene nanoplatelets in ~100% yield, ACS Nano 10 (1) (2016) 274–279.
[10] X. Geng, Y. Guo, D. Li, W. Li, C. Zhu, X. Wei, M. Chen, S. Gao, S. Qiu, Y. Gong, et al., Interlayer catalytic exfoliation realizing scalable production of large-size pristine few-layer graphene, Sci. Rep. 3 (2013) 2013, http://dx.doi.org/10.1038/srep01134.
[11] F. Xiang, R. Mukherjee, J. Zhong, Y. Xia, N. Gu, Z. Yang, N. Koratkar, Scalable and rapid far infrared reduction of graphene oxide for high performance lithium ion batteries, Energy Storage Mater. 1 (2015) 9–16.
[12] S. Ichinokura, K. Sugawara, A. Takayama, T. Takahashi, S. Hasegawa, Superconducting calcium-intercalated bilayer graphene, ACS Nano 10 (2) (2016) 2761–2765.
[13] S.L. Yang, J.A. Sobota, C.A. Howard, C.J. Pickard, M. Hashimoto, D.H. Lu, S.K. Mo, P.S. Kirchmann, Z.X. Shen, Superconducting graphene sheets in CaC_6enabled by phonon-mediated interband interactions, Nat. Commun. 5 (3493) (2014), http://dx.doi.org/10.1038/ncomms4493.
[14] T.E. Weller, M. Ellerby, S.S. Saxena, R.P. Smith, N.T. Skipper, Superconductivity in the intercalated graphite compounds C_6Yb and C_6Ca, Nat. Phys. 1 (2005) 39–41.
[15] L.M. Viculis, J.J. Mack, O.M. Mayer, H.T. Hahn, R.B. Kaner, Intercalation and exfoliation routes to graphite nanoplatelets, J. Mater. Chem. 15 (9) (2005) 974–978.
[16] M. Matsumoto, Y. Saito, C. Park, T. Fukushima, T. Aida, Ultrahigh-throughput exfoliation of graphite into pristine 'single-layer' graphene using microwaves and molecularly engineered ionic liquids, Nat. Chem. 7 (2015) 730–736.
[17] Y. Zhu, S. Murali, M.D. Stoller, A. Velamakanni, R.D. Piner, R.S. Ruoff, Microwave assisted exfoliation and reduction of graphite oxide for ultracapacitors, Carbon 48 (7) (2010) 2118–2122.
[18] Y. Kim, E.-s. Cho, S.-J. Park, S. Kim, One-pot microwave-assisted synthesis of reduced graphene oxide/nickel cobalt double hydroxide composites and their electrochemical behavior, J. Ind. Eng. Chem. 33 (2016) 108–114.
[19] A.P. Cohn, K. Share, R. Carter, L. Oakes, C.L. Pint, Ultrafast solvent-assisted sodium ion intercalation into highly crystalline few-layered graphene, Nano Lett. 16 (1) (2016) 543–548.
[20] H.L. Poh, P. Šimek, Z. Sofer, M. Pumera, Sulfur-doped graphene via thermal exfoliation of graphite oxide in H_2S, SO_2, or CS_2 gas, ACS Nano 7 (6) (2013) 5262–5272.
[21] C.H.A. Wong, Z. Sofer, K. Klímová, M. Pumera, Microwave exfoliation of graphite oxides in H_2S plasma for the synthesis of sulfur-doped graphenes as oxygen reduction catalysts, ACS Appl. Mater. Interfaces 8 (46) (2016) 31849–31855.
[22] G. Hasegawa, T. Deguchi, K. Kanamori, Y. Kobayashi, H. Kageyama, T. Abe, K. Nakanishi, High-level doping of nitrogen, phosphorus, and sulfur into activated carbon monoliths and their electrochemical capacitances, Chem. Mater. 27 (13) (2015) 4703–4712.
[23] G. Csanyi, P.B. Littlewood, A.H. Nevidomskyy, C.J. Pickard, B.D. Simons, The role of the interlayer state in the electronic structure of superconducting graphite intercalated compounds, Nat. Phys. 1 (1) (2005) 42–45.
[24] R.A. Jishi, M. Dresselhaus, Superconductivity in graphite intercalation compounds, Phys. Rev. B 45 (21) (1992) 12465–12469.
[25] O. Jankovský, V. Mazánek, K. Klímová, D. Sedmidubský, J. Kosina, M. Pumera, Z. Sofer, Simple synthesis of fluorinated graphene: thermal exfoliation of fluorographite, Chem. Eur. J. 22 (49) (2016) 17696–17703.
[26] M. Ujihara, M.M.M. Ahmed, T. Imae, Y. Yamauchi, Massive-exfoliation of magnetic graphene from acceptor-type GIC by long-chain alkyl amine, J. Mater. Chem. A 2 (2014) 4244–4250.
[27] M.M.M. Ahmed, T. Imae, Electrochemical properties of a thermally expanded magnetic graphene composite with a conductive polymer, Phys. Chem. Chem. Phys. 18 (2016) 10400–10410.
[28] L.K. Shrestha, R.G. Shrestha, Y. Yamauchi, J.P. Hill, T. Nishimura, K. Miyazawa, T. Kawai, S. Okada, K. Wakabayashi, K. Ariga, Nanoporous carbon tubes from fullerene crystals as the π-electron carbon source, Angew. Chem. Int. Ed. 54 (3) (2015) 951–955.
[29] Y. Zhu, S. Murali, M.D. Stoller, K.J. Ganesh, W. Cai, P.J. Ferreira, et al., Carbon-based supercapacitors produced by activation of graphene, Science 332 (6037) (2011) 1537–1541.
[30] J. Zhang, H. Zhu, M. Wang, W. Wang, Z. Chen, Electrochemical determination of sunset yellow based on an expanded graphite paste electrode, J. Electrochem. Soc. 160 (8) (2013) H459–H462.
[31] S. Paszkiewicz, A. Szymczyk, Z. Špitalský, J. Mosnáček, Z. Rosłaniec, Morphology and thermal properties of expanded graphite (EG)/polyethylene terephthalate (PET) nanocomposites, CHEMIK 1 (66) (2012) 21–30.
[32] Q.-L. Yan, M. Gozin, F.-Q. Zhao, A. Cohen, S.-P. Pang, Highly energetic compositions based on functionalized carbon nanomaterials, Nanoscale 8 (9) (2016) 4799–4851.
[33] J. -h. Li, L. -l. Feng, Z. -x. Jia, Preparation of expanded graphite with 160 μm mesh of fine flake graphite, Mater. Lett. 60 (6) (2006) 746–749.
[34] S. Gambhir, R. Jalili, D.L. Officer, G.G. Wallace, Chemically converted graphene: scalable chemistries to enable processing and fabrication, NPG Asia Mater. 7 (2015) e186, http://dx.doi.org/10.1038/am.2015.47.
[35] G. Carotenuto, A. Longo, L. Nicolais, S. De Nicola, E. Pugliese, M. Ciofini, M. Locatelli, A. Lapucci, R. Meucci, Laser-induced thermal expansion of H_2SO_4-intercalated graphite lattice, J. Phys. Chem. C 119 (28) (2015) 15942–15947.
[36] X.-X. Wu, H.-X. Li, G.-Q. Liu, C.-C. Niu, G. Wang, J.-L. Sun, Nanocarbon-coated α-Al_2O_3 composite powders synthesized by high-energy ball milling, J. Inorg. Mater. 28 (3) (2013) 261–266.
[37] M. Zhou, T. Tian, X. Li, X. Sun, J. Zhang, P. Cui, J. Tang, L.-C. Qin, Production of graphene by liquid-phase exfoliation of intercalated graphite, Int. J. Electrochem. Sci. 9 (2014) 810–820.
[38] M. Khan, M.N. Tahir, S.F. Adil, H.U. Khan, M.R.H. Siddiqui, A.A. Al-warthan, W. Tremel, Graphene based metal and metal oxide nanocomposites: synthesis, properties and their applications, J. Mater. Chem. A 3 (37) (2015) 18753–18808.
[39] S. Lin, L. Dong, J. Zhang, H. Lu, Room-temperature intercalation and ~ 1000-fold chemical expansion for scalable preparation of high-quality graphene, Chem. Mater. 28 (7) (2016) 2138–2146.
[40] K.H. Park, D. Lee, J. Kim, J. Song, Y.M. Lee, H.-T. Kim, J.-K. Park, Defect-free, size-tunable graphene for high-performance lithium ion battery, Nano Lett. 14 (8) (2014) 4306–4313.
[41] K.H. Lee, J. Oh, J.G. Son, H. Kim, S.-S. Lee, Nitrogen-doped graphene nanosheets from bulk graphite using microwave irradiation, ACS Appl. Mater. Interfaces 6 (9) (2014) 6361–6368.
[42] P. Bairi, R.G. Shrestha, J.P. Hill, T. Nishimura, K. Ariga, L.K. Shrestha, Mesoporous graphitic carbon microtubes derived from fullerene C 70 tubes as a high performance electrode material for advanced supercapacitors, J. Mater. Chem. A 4 (36) (2016) 13899–13906.
[43] D. Graf, F. Molitor, K. Ensslin, C. Stampfer, A. Jungen, C. Hierold, L. Wirtz, Spatially resolved Raman spectroscopy of single-and few-layer graphene, Nano Lett. 7 (2) (2007) 238–242.
[44] X. Qi, H.-B. Zhang, J. Xu, X. Wu, D. Yang, J. Qu, Z.-Z. Yu, Highly efficient high-pressure homogenization approach for scalable production of high-quality graphene sheets and sandwich-structured α-Fe_2O_3/graphene hybrids for high-performance lithium-ion batteries, ACS Appl. Mater. Interfaces 9 (12) (2017) 11025–11034.
[45] K. Li, J. Liu, Y. Huang, F. Bu, Y. Xu, Integration of ultrathin graphene/polyaniline composite nanosheets with a robust 3D graphene framework for highly flexible all-solid-state supercapacitors with superior energy density and exceptional cycling stability, J. Mater. Chem. A 5 (11) (2017) 5466–5474.
[46] T. Liu, L. Finn, M. Yu, H. Wang, T. Zhai, X. Lu, et al., Polyaniline and polypyrrole pseudocapacitor electrodes with excellent cycling stability, Nano Lett. 14 (5) (2014) 2522–2527.
[47] A. Moyseowicz, A. Śliwak, E. Miniach, G. Gryglewicz, Polypyrrole/iron oxide/reduced graphene oxide ternary composite as a binderless electrode material with high cyclic stability for supercapacitors, Compos. Part B: Eng. 109 (2017) 23–29.
[48] X. Hong, B. Zhang, E. Murphy, J. Zou, F. Kim, Three-dimensional reduced graphene oxide/polyaniline nanocomposite film prepared by diffusion driven layer-by-layer assembly for high-performance supercapacitors, J. Power Sources 343 (2017) 60–66.